



**UNIVERSIDAD DE INVESTIGACION DE
TECNOLOGIA EXPERIMENTAL YACHAY**

Escuela de Ciencias Físicas y Nanotecnología

**TÍTULO: First Principles and Machine Learning
Investigations into the Atomic and Mechanical
Properties of Cement Hydrates (C-S-H).**

Trabajo de integración curricular presentado como requisito para
la obtención del título de Físico

Autor:

Balarezo J. Gabriel

Tutor:

Ph.D - Pinto Henry

Urcuquí, Junio 2025

AUTORÍA

Yo, **Balarezo Balarezo Juan Gabriel**, con cédula de identidad 0106019219, declaro que las ideas, juicios, valoraciones, interpretaciones, consultas bibliográficas, definiciones y conceptualizaciones expuestas en el presente trabajo; así cómo, los procedimientos y herramientas utilizadas en la investigación, son de absoluta responsabilidad de el/la autora (a) del trabajo de integración curricular. Así mismo, me acojo a los reglamentos internos de la Universidad de Investigación de Tecnología Experimental Yachay.

Urcuquí, junio 2025.

Juan Gabriel Balarezo Balarezo

C.I: 0106019219

AUTORIZACIÓN DE PUBLICACIÓN

Yo, **Balarezo Balarezo Juan Gabriel**, con cédula de identidad 0106019219, cedo a la Universidad de Investigación de Tecnología Experimental Yachay, los derechos de publicación de la presente obra, sin que deba haber un reconocimiento económico por este concepto. Declaro además que el texto del presente trabajo de titulación no podrá ser cedido a ninguna empresa editorial para su publicación u otros fines, sin contar previamente con la autorización escrita de la Universidad.

Asimismo, autorizo a la Universidad que realice la digitalización y publicación de este trabajo de integración curricular en el repositorio virtual, de conformidad a lo dispuesto en el Art. 144 de la Ley Orgánica de Educación Superior

Urcuquí, junio 2025.

Juan Gabriel Balarezo Balarezo
C.I: 0106019219

For her, who is my everything.
For my family, who always supported me.

Balarezo J. Gabriel

Acknowledgments

Me gustaría expresar mi más sincero agradecimiento a mis padres, cuyo apoyo incondicional y aliento han sido la fuerza impulsora detrás de mi trayectoria académica, y cuyos sacrificios y confianza en mí han sido fundamentales para alcanzar este logro. A la Gnosis por enseñarme a mejorar como ser humano. A mis amigos, cuya compañía y amistad han traído alegría y risas en cada paso de este camino, gracias por siempre estar ahí. Un agradecimiento especial a mi novia, cuyo amor, comprensión y paciencia han sido una fuente constante de fortaleza e inspiración, siendo mi roca en los diversos desafíos. Me siento increíblemente afortunado de haber recibido la guía y el apoyo incondicional de mis co-asesores, María Camila y el Profesor Andrés, cuya experiencia, mentoría y dedicación han sido invaluable para la realización de esta tesis. Extiendo mi gratitud al mejor profesor de Yachay Tech, Henry Pinto.

Finalmente, dedico esta tesis a mi abuelo, cuya resiliencia y fortaleza frente a la adversidad han sido una fuente de inspiración. Su amor y sabiduría me han guiado a lo largo de los altibajos de la vida, y estoy eternamente agradecido por su presencia en mi vida.

Balarezo J. Gabriel

Resumen

Este estudio presenta una investigación exhaustiva de las propiedades magnéticas y electrónicas de los monocapas $X\text{GeTe}_3$ ($X = \text{Cr}, \text{Mn}, \text{Fe}$) y sus aleaciones aleatorias, utilizando la teoría del funcional de la densidad (DFT) con los funcionales PBE y PBEsol, complementados con correcciones de Hubbard U . CrGeTe_3 exhibe un robusto orden ferromagnético (FM) con una brecha de banda calculada que concuerda bien con los datos experimentales, destacando su potencial para aplicaciones prácticas. La monocapa MnGeTe_3 muestra un comportamiento de medio metal (HM), lo que lo hace particularmente prometedor para aplicaciones espintrónicas. En contraste, FeGeTe_3 revela un estado fundamental antiferromagnético (AFM) y posibles inestabilidades dinámicas, lo que requiere una mayor exploración para optimizar sus propiedades electrónicas.

En las aleaciones aleatorias, se observaron modificaciones significativas en los momentos magnéticos y las estructuras electrónicas. Específicamente, en $\text{Cr}_{1-x}\text{GeMn}_x\text{Te}_3$, el desorden en el momento magnético sugiere estados magnéticos fundamentales complejos, beneficiosos para la espintrónica. Mientras tanto, $\text{Cr}_{1-x}\text{GeFe}_x\text{Te}_3$ demuestra efectos de fuerte hibridación, indicando su idoneidad para sensores magnéticos y aplicaciones termoeléctricas. El sistema $\text{Fe}_{1-x}\text{GeMn}_x\text{Te}_3$ revela desafíos estructurales a mayores concentraciones de Mn, pero su estabilidad termodinámica respalda su potencial uso en uniones túnel magnéticas.

En general, esta investigación resalta las considerables perspectivas tecnológicas de los monocapas $X\text{GeTe}_3$ y sus aleaciones aleatorias, abogando por un control preciso de las propiedades magnéticas y electrónicas para avanzar en sus aplicaciones en espintrónica, memorias magnéticas y dispositivos termoeléctricos.

Palabras clave: Teoría del Funcional de la Densidad, monocapas, ferromagnetismo, anti-ferromagnetismo, semi-metal, aleaciones aleatorias.

Abstract

This study presents a thorough investigation of the magnetic and electronic properties of $X\text{GeTe}_3$ ($X = \text{Cr}, \text{Mn}, \text{Fe}$) monolayers and their random alloys, utilizing density functional theory (DFT) with PBE and PBEsol functionals, supplemented by Hubbard U corrections. CrGeTe_3 exhibits robust ferromagnetic (FM) ordering with a calculated band gap that aligns well with experimental data, highlighting its potential for practical applications. The MnGeTe_3 monolayer shows half-metallic (HM) behavior, making it particularly promising for spintronic applications. In contrast, FeGeTe_3 reveals an antiferromagnetic (AFM) ground state and potential dynamical instabilities, necessitating further exploration to optimize its electronic properties.

For the random alloys, significant modifications in magnetic moments and electronic structures were noted. Specifically, in $\text{Cr}_{1-x}\text{GeMn}_x\text{Te}_3$, magnetic moment disorder suggests complex magnetic ground states beneficial for spintronics. Meanwhile, $\text{Cr}_{1-x}\text{GeFe}_x\text{Te}_3$ demonstrates strong hybridization effects, indicating its suitability for magnetic sensors and thermoelectric applications. The $\text{Fe}_{1-x}\text{GeMn}_x\text{Te}_3$ system reveals structural challenges at higher Mn concentrations, but its thermodynamic stability supports its potential use in magnetic tunneling junctions.

Overall, this research emphasizes the considerable technological prospects of $X\text{GeTe}_3$ monolayers and their random alloys, advocating for precise control over magnetic and electronic properties to advance their applications in spintronics, magnetic memory, and thermoelectric devices.

Keywords: Density Functional Theory, monolayers, ferromagnetism, anti-ferromagnetism, half-metal, random alloys.

Contents

Contents	vii
List of Figures	ix
List of Tables	x
1 Introduction	1
1.1 Background	1
1.2 Problem Statement	2
1.3 General and Specific Objectives	2
1.4 Overview	2
2 Theoretical Background	4
2.1 Many Body Schrödinger Equation	4
2.1.1 The Coulomb Interaction	4
2.1.2 The Time-Independent Schrödinger Equation	5
2.2 The Born-Oppenheimer Approximation	7
2.3 Hartree-Fock Approximation	8
2.3.1 The Pauli Exclusion Principle	10
2.3.2 The Hartree-Fock Equations	10
2.4 Density Functional Theory	11
2.4.1 First Hohenberg-Kohn Theorem	12
2.4.2 Second Hohenberg-Kohn Theorem	12
2.4.3 Kohn-Sham Equations	12
2.4.4 Exchange-Correlation Functionals	12
2.5 Ab initio Molecular Dynamics	12
2.5.1 Born-Oppenheimer Molecular Dynamics	12
2.5.2 Car-Parrinello Molecular Dynamics	12
2.6 Machine Learning Force Fields	12
2.7 Computational Implementation in VASP	12
2.7.1 Plane Wave Basis Set	12
2.7.2 K-Point Sampling and Cutoff Energy	12
2.7.3 Pseudopotentials	12
2.8 Density of States	12
3 Methodology	13
4 Results & Discussion	14

4.1 My results	14
--------------------------	----

Bibliography	15
---------------------	-----------

List of Figures

1.1	A four-level model representing the upscaling of C-S-H properties from the nanoscale to the engineering scale. (a) snapshot of C-S-H's nanostructure. (b) microstructure of C-S-H created by agglomeration of randomly oriented C-S-H nanoparticles. (c) microtexture of hardened paste composed by hydration products. (d) macrotexture of cement paste at the engineering scale. Adapted from ⁹	2
4.1	A schematic representation of the DFT formalism. The many-body wavefunction is replaced by a single-particle wavefunction, which is used to calculate the electron density. The electron density is then used to calculate the total energy of the system. Adapted from ¹⁰	14

List of Tables

Chapter 1

Introduction

1.1 Background

Concrete is the synthetic material currently produced in volumes larger than any other material on Earth. With an annual consumption of approximately 35 billion tonnes, it is only second to water in terms of global usage^{1,2}. As the backbone of modern infrastructure, it provides the foundations for buildings, bridges, roads, dams, and other structures essential for societal development. Its widespread adoption arises from a unique combination of strength, versatility, and cost-effectiveness³, rendering it indispensable to the construction industry.

Nevertheless, despite the ubiquity of concrete, the properties of its key constituent, cement, remain incompletely understood. Cement is a chemically complex material, composed of a heterogeneous mixture of minerals that undergo a series of hydration reactions upon contact with water. The principal product of cement hydration—and the primary binding phase of concrete—calcium silicate hydrate (C-S-H)¹ is the responsible for the mechanical strength, chemical and transport properties and durability of hardened cement paste and, consequently, of concrete itself^{4,5,6,7}. Therefore, understanding the atomic and mechanical properties of C-S-H is of the uttermost importance to better formulate cementitious materials with enhanced performance and durability.⁸

¹Cement chemistry nomenclature

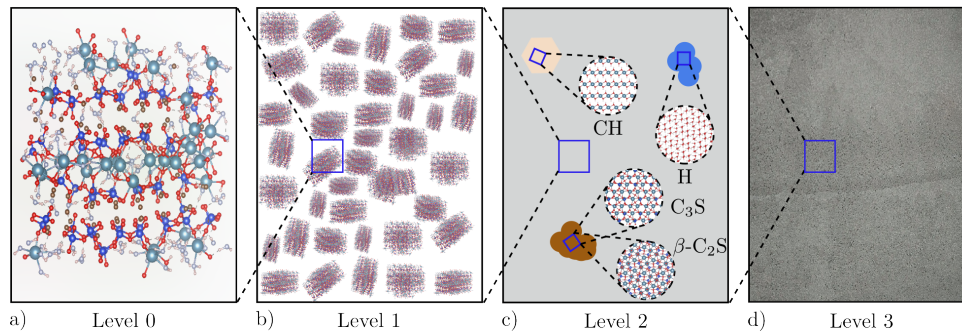


Figure 1.1: A four-level model representing the upscaling of C-S-H properties from the nanoscale to the engineering scale. (a) snapshot of C-S-H's nanostructure. (b) microstructure of C-S-H created by agglomeration of randomly oriented C-S-H nanoparticles. (c) microtexture of hardened paste composed by hydration products. (d) macrotexture of cement paste at the engineering scale. Adapted from⁹.

1.2 Problem Statement

Nunc posuere quam at lectus tristique eu ultrices augue venenatis. Vestibulum ante ipsum primis in faucibus orci luctus et ultrices posuere cubilia Curae; Aliquam erat volutpat. Vivamus sodales tortor eget quam adipiscing in vulputate ante ullamcorper. Sed eros ante, lacinia et sollicitudin et, aliquam sit amet augue. In hac habitasse platea dictumst.

1.3 General and Specific Objectives

Morbi rutrum odio eget arcu adipiscing sodales. Aenean et purus a est pulvinar pellentesque. Cras in elit neque, quis varius elit. Phasellus fringilla, nibh eu tempus venenatis, dolor elit posuere quam, quis adipiscing urna leo nec orci. Sed nec nulla auctor odio aliquet consequat. Ut nec nulla in ante ullamcorper aliquam at sed dolor. Phasellus fermentum magna in augue gravida cursus. Cras sed pretium lorem. Pellentesque eget ornare odio. Proin accumsan, massa viverra cursus pharetra, ipsum nisi lobortis velit, a malesuada dolor lorem eu neque.

1.4 Overview

Sed ullamcorper quam eu nisl interdum at interdum enim egestas. Aliquam placerat justo sed lectus lobortis ut porta nisl porttitor. Vestibulum mi dolor, lacinia molestie gravida at, tempus vitae ligula. Donec eget quam sapien, in viverra eros. Donec pellentesque justo a massa fringilla non vestibulum metus vestibulum. Vestibulum in orci quis felis tempor lacinia. Vivamus ornare ultrices facilisis. Ut hendrerit volutpat vulputate. Morbi condimentum venenatis augue, id porta ipsum vulputate in. Curabitur luctus tempus justo. Vestibulum risus lectus, adipiscing nec condimentum quis, condimentum nec nisl. Aliquam dictum sagittis velit sed iaculis. Morbi

tristique augue sit amet nulla pulvinar id facilisis ligula mollis. Nam elit libero, tincidunt ut aliquam at, molestie in quam. Aenean rhoncus vehicula hendrerit.

Chapter 2

Theoretical Background

This chapter is devoted to present the theoretical foundations and formalism of Density Functional Theory (DFT) and related methods required for the development of the results presented in this work. Starting with the many-body Schrödinger equation, this chapter covers the Born-Oppenheimer approximation, the Hartree-Fock approximation, Hohenberg-Kohn theorems, the Kohn-Sham equations, exchange-correlation functionals, and definitions on Ab initio molecular dynamics (AIMD) and machine learning force fields (MLFFs), along with implementation details in the Vienna Ab initio Simulation Package (VASP).

Ultimately, the aim of this chapter is to provide a comprehensive understanding of the theoretical framework that underpins the computational methods utilised in this work, enabling the reader to grasp the principles and assumptions that govern the simulations and analyses performed throughout.

2.1 Many Body Schrödinger Equation

In the realm of materials science, comprehending particle behaviour within a system inevitably demands resorting to intricate principles of quantum mechanics. Our journey shall commence by describing the physical laws that shape the interactions among particles constituting a system—electrons and nuclei alike.

2.1.1 The Coulomb Interaction

Materials may be thought of as complex assemblies of electrons and nuclei, held together by a delicate balance between attractive Coulomb interactions—primarily between electrons and nuclei—and repulsive interactions between like-charged particles, such as electron-electron and

nucleus-nucleus pairs, which govern the overall dynamics of the material system^{10,11,12}. From classical electrostatics, these interactions can be mathematically expressed as follows:

- Electron-electron interactions

$$\hat{V}_{ee} = \frac{1}{2} \sum_{i \neq j} \frac{e^2}{4\pi\epsilon_0 |\mathbf{r}_i - \mathbf{r}_j|} \quad (2.1)$$

- Electron-nucleus interactions

$$\hat{V}_{nn} = \frac{1}{2} \sum_{I \neq J} \frac{e^2}{4\pi\epsilon_0} \frac{Z_I Z_J}{|\mathbf{R}_I - \mathbf{R}_J|} \quad (2.2)$$

- Electron-nuclei interactions

$$\hat{V}_{en} = - \sum_{i \neq I} \frac{e^2}{4\pi\epsilon_0} \frac{Z_I}{|\mathbf{r}_i - \mathbf{R}_I|} \quad (2.3)$$

where e is the electronic charge, ϵ_0 is the vacuum permittivity, Z_I and Z_J are the atomic numbers of nuclei I and J , respectively, and \mathbf{r}_i and \mathbf{R}_I are the position vectors of electrons and nuclei, respectively. Moreover, we must also consider the kinetic energy of the collection of electrons and nuclei

$$\hat{T} = - \sum_i \frac{\hbar^2}{2m_e} \nabla_i^2 - \sum_I \frac{\hbar^2}{2M_I} \nabla_I^2 \quad (2.4)$$

where \hbar is the reduced Planck's constant, m_e is the electron mass, and M_I is the mass of the nucleus I .

2.1.2 The Time-Independent Schrödinger Equation

The Time-Independent Schrödinger Equation (TISE) lies at the heart of non-relativistic quantum mechanics, providing a mathematical framework to describe stationary electronic states of quantum systems. It takes the following form:

$$\hat{H}\psi(\mathbf{r}) = E\psi(\mathbf{r}) \quad (2.5)$$

where \hat{H} is the Hamiltonian of the system, encompassing both kinetic and potential energies, $\psi(\mathbf{r})$ is the wavefunction of the system, and E is the energy eigenvalue associated with the state described by $\psi(\mathbf{r})$. It is important to note that Equation 2.5 is applicable to a single particle, yet a material system is composed of many electrons (N) and nuclei (M) with spatial coordinates $\mathbf{r}_1, \mathbf{r}_2, \dots, \mathbf{r}_N$ and $\mathbf{R}_1, \mathbf{R}_2, \dots, \mathbf{R}_M$, respectively. Therefore, we must introduce a so

called many-body wavefunction given by:

$$\Psi(\mathbf{r}_1, \mathbf{r}_2, \dots, \mathbf{r}_N, \mathbf{R}_1, \mathbf{R}_2, \dots, \mathbf{R}_M) \quad (2.6)$$

On this basis, the many-body version of Equation 2.5 shall be constructed by combining the kinetic (Equation 2.4) and potential (Equations 2.1, 2.2, and 2.3) energy contributions, leading to the following expression:

$$\left[-\sum_i \frac{\hbar^2}{2m_e} \nabla_i^2 - \sum_I \frac{\hbar^2}{2M_I} \nabla_I^2 + \frac{1}{2} \sum_{i \neq j} \frac{e^2}{4\pi\epsilon_0 |\mathbf{r}_i - \mathbf{r}_j|} + \frac{1}{2} \sum_{I \neq J} \frac{e^2}{4\pi\epsilon_0 |\mathbf{R}_I - \mathbf{R}_J|} - \sum_{i,I} \frac{e^2}{4\pi\epsilon_0 |\mathbf{r}_i - \mathbf{R}_I|} \right] \Psi = E_{\text{tot}} \Psi \quad (2.7)$$

Equation 2.7 provides a complete description of the stationary states of a non-relativistic many-body system, under time-independent conditions and in the absence of external fields. Additionally, we can achieve a more compact formulation by introducing the concept of atomic units. To this end, let us consider the simplest electron-nucleus system—the hydrogen atom—where the electron orbital has an average radius $a_0 \approx 0.529 \text{ \AA}$. Thereby, the Coulomb energy for such a system is given by:

$$E_{\text{Ha}} = \frac{e^2}{4\pi\epsilon_0 a_0} \quad (2.8)$$

where 'Ha' stands for Hartree. Within this framework, the Hartree energy represents the Coulomb interaction between two fundamental charges separated by a distance of one Bohr radius (a_0). Moreover, the angular momentum quantisation condition for the electron in the hydrogen atom is given by

$$m_e v a_0 = \hbar \quad (2.9)$$

Additionally, the equilibrium condition between the nuclear attraction and the electron's centrifugal force can be expressed as:

$$\frac{e^2}{4\pi\epsilon_0 a_0^2} = \frac{m_e v^2}{a_0} \quad (2.10)$$

By combining Equations 2.8, 2.9, and 2.10, we derive the following relationships:

$$\frac{e^2}{4\pi\epsilon_0 a_0} = \frac{\hbar^2}{m_e a_0^2} \quad (2.11)$$

$$\frac{1}{2} m_e v^2 = \frac{1}{2} E_{\text{Ha}} \quad (2.12)$$

This latter relation showcases that the kinetic energy is of the same order as E_{Ha} , rendering it convenient to normalise Equation 2.7 by this quantity:

$$\left[-\sum_i \frac{1}{2} a_0^2 \nabla_i^2 - \sum_I \frac{1}{2} \frac{1}{(M_I/m_e)} \nabla_I^2 + \frac{1}{2} \sum_{i \neq j} \frac{a_0}{|\mathbf{r}_i - \mathbf{r}_j|} + \frac{1}{2} \sum_{I \neq J} \frac{Z_I Z_J}{|\mathbf{R}_I - \mathbf{R}_J|} - \sum_{i,I} \frac{Z_I}{|\mathbf{r}_i - \mathbf{R}_I|} \right] \Psi = \frac{E_{\text{tot}}}{E_{\text{Ha}}} \Psi \quad (2.13)$$

A final simplification involves setting our energy units to Ha, distance units to a_0 , and mass units to m_e . The last missing constant e is set to 1, leading to the following expression:

$$\left[-\sum_i \frac{\nabla_i^2}{2} - \sum_I \frac{\nabla_I^2}{2M_I} + \frac{1}{2} \sum_{i \neq j} \frac{1}{|\mathbf{r}_i - \mathbf{r}_j|} + \frac{1}{2} \sum_{I \neq J} \frac{Z_I Z_J}{|\mathbf{R}_I - \mathbf{R}_J|} - \sum_{i,I} \frac{Z_I}{|\mathbf{r}_i - \mathbf{R}_I|} \right] \Psi = E_{\text{tot}} \Psi \quad (2.14)$$

Ultimately, even though Equation 2.14 provides an exact method capable of yielding various properties of a material system—such as elastic, thermal, and electronic properties—a combination of mathematical complexity and computational limitations renders it intractable to solve for any realistic system. Moreover, the wavefunction contains vastly more information than is necessary to describe most observable properties of a material. Therefore, we must resort to alternative formulations that allow us to extract only the relevant information from the wavefunction whilst reducing the computational cost of the calculations. The remainder of this chapter is dedicated to presenting such alternative approaches that ultimately lead to the computational methods employed throughout this work.

2.2 The Born-Oppenheimer Approximation

For atoms in a solid, we can think of nuclei as being held immobile in a fixed position, while electrons instantaneously react to any nuclei movement. This assumption is based on the fact that nuclei are much heavier than electrons—by three to four orders of magnitude—making the former behave like classical particles. Thereby, we can rewrite the many-body wavefunction as a product of two wavefunctions:

$$\Psi(\mathbf{r}_1, \mathbf{r}_2, \dots, \mathbf{r}_N, \mathbf{R}_1, \mathbf{R}_2, \dots, \mathbf{R}_M) = \psi_{\mathbf{R}}(\mathbf{r}_1, \mathbf{r}_2, \dots, \mathbf{r}_N) \chi(\mathbf{R}) \quad (2.15)$$

where $\psi_{\mathbf{R}}$ is the electronic wavefunction parametrised by the nuclear positions \mathbf{R} , and χ is the nuclear wavefunction. Furthermore, this significant mass disparity enables a systematic

approximation scheme, in which the electronic wavefunction is solved for fixed nuclei, and its solution is used as an effective potential for the nuclear dynamics afterwards. First, nuclei kinetic energy is neglected, as their positions are assumed to be fixed:

$$\sum_I \frac{\nabla_I^2}{2M_I} = 0 \quad \text{and} \quad E = E_{\text{tot}} - \sum_{I < J} \frac{Z_I Z_J}{|\mathbf{R}_I - \mathbf{R}_J|} \quad (2.16)$$

Following, we define the Coulomb potential of the nuclei experienced by the electrons as:

$$V_n(\mathbf{r}) = - \sum_I \frac{Z_I}{|\mathbf{r} - \mathbf{R}_I|} \quad (2.17)$$

Then, Equation 2.14 can be rewritten as:

$$\left[- \sum_i \frac{\nabla_i^2}{2} + \sum_i V_n(\mathbf{r}_i) + \frac{1}{2} \sum_{i \neq j} \frac{1}{|\mathbf{r}_i - \mathbf{r}_j|} \right] \Psi = E \Psi \quad (2.18)$$

Finally, by using Equation 2.15, we can define the electronic and nuclear Schrödinger equations as follows:

$$\left[- \sum_i \frac{\nabla_i^2}{2} + \sum_i V_n(\mathbf{r}_i) + \frac{1}{2} \sum_{i \neq j} \frac{1}{|\mathbf{r}_i - \mathbf{r}_j|} \right] \psi_{\mathbf{R}} = E_{\mathbf{R}} \psi_{\mathbf{R}} \quad (2.19)$$

$$\left[- \sum_I \frac{\nabla_I^2}{2M_I} + \sum_{I < J} \frac{Z_I Z_J}{|\mathbf{R}_I - \mathbf{R}_J|} + E(\mathbf{R}_1, \dots, \mathbf{R}_M) \right] \chi(\mathbf{R}) = E_{\text{tot}} \chi(\mathbf{R}) \quad (2.20)$$

where $E_{\mathbf{R}} = E(\mathbf{R}_1, \dots, \mathbf{R}_M)$ is the electronic surface energy, which is a function of the nuclear positions, and serves as an effective potential shaping the nuclear dynamics.

2.3 Hartree-Fock Approximation

The essence of the Hartree-Fock approximation (HFA) is approximate the interacting many-electron system (Equation 2.18) by a set of non-interacting single-particle problems subject to an effective mean-field potential^{13,14,15}. As a means to this, we first rewrite the total wavefunction for a system with N electrons as the product of single-electron wavefunctions—often referred to as the Hartree approximation¹⁶—as showcased in Equation 2.21.

$$\Psi^H(\mathbf{r}_1, \dots, \mathbf{r}_N) = \prod_{i=1}^N \phi_i(\mathbf{r}_i) \quad (2.21)$$

Following, we construct the total energy functional as the expectation value of the Hamiltonian operator:

$$E^H[\{\phi_i\}] = \left\langle \Psi^H \left| \hat{H} \right| \Psi^H \right\rangle \quad (2.22)$$

Expanding Equation 2.22:

$$E^H[\{\phi_i\}] = \sum_{i=1}^N \int \phi_i^*(\mathbf{r}) \left(-\frac{\nabla^2}{2} + V_n(\mathbf{r}) \right) \phi_i(\mathbf{r}) d\mathbf{r} + \frac{1}{2} \sum_{i \neq j} \int \int \frac{|\phi_i(\mathbf{r})|^2 |\phi_j(\mathbf{r}')|^2}{|\mathbf{r} - \mathbf{r}'|} d\mathbf{r} d\mathbf{r}' \quad (2.23)$$

where the first term adds up the kinetic energy and electron-nuclear attraction overall electrons, whilst the second accounts for the classical electron-electron repulsion energy averaged over the electron density distribution. In order to find the set of orbitals $\{\phi_i\}$ that minimises the total energy functional we use the variational principle where we shall impose the orthonormality condition:

$$\int \phi_i^*(\mathbf{r}) \phi_j(\mathbf{r}) d\mathbf{r} = \delta_{ij} \quad (2.24)$$

for what we introduce the Lagrange multipliers λ_{ij} to enforce these constraints and define the Lagrangian:

$$\mathcal{L} = E^H[\{\phi_i\}] - \sum_{i=1}^N \lambda_{ij} (\langle \phi_i | \phi_j \rangle - \delta_{ij}) \quad (2.25)$$

which ultimately simplifies to:

$$\mathcal{L} = E^H[\{\phi_i\}] - \sum_{i=1}^N \varepsilon_i (\langle \phi_i | \phi_i \rangle - 1) \quad (2.26)$$

Then, we need to compute the derivative of \mathcal{L} with respect to ϕ_i^* and set it to zero:

$$\frac{\delta \mathcal{L}}{\delta \phi_i^*}(\mathbf{r}) = 0 \quad (2.27)$$

which yield to the Hartree equation:

$$\left[-\frac{\nabla^2}{2} + V_n(\mathbf{r}) + V_i^H(\mathbf{r}) \right] \phi_i(\mathbf{r}) = \varepsilon_i \phi_i(\mathbf{r}) \quad (2.28)$$

where $V_n(\mathbf{r})$ represents the electrostatic interaction between electrons and nuclei, and the Hartree potential

$$V_i^H(\mathbf{r}) = \sum_{j \neq i} \int \frac{|\phi_j(\mathbf{r}')|^2}{|\mathbf{r} - \mathbf{r}'|} d\mathbf{r}' \quad (2.29)$$

accounts for the average electrostatic interaction experienced by the i -th electron due to all other electrons in the system. This effective mean-field potential replaces the electron-electron interactions, effectively simplifying the many-body problem into single-particle problems.

2.3.1 The Pauli Exclusion Principle

So far, we have introduced the Hartree approximation, which assumes that the many-electron wavefunction can be expressed as a product of single-particle wavefunctions. However, this approach does not account for the indistinguishability of electrons and the Pauli exclusion principle, which states that no two fermions—half spin particles, such as electrons—can reside in the same quantum state simultaneously. In doing so, it imposes a restriction on the possible configurations of electrons in a system that shall be accounted for.

In order to achieve this, V. Fock¹⁷ introduced a different approximation to the wavefunction by using a Slater determinant—a mathematical construct that combines one-electron wavefunctions in such a way that satisfies the antisymmetry principle. This is done by expressing the overall wavefunction as the determinant of a matrix of single-electron wavefunctions:

$$\Psi^{HF}(\mathbf{r}_1, \dots, \mathbf{r}_N) = \frac{1}{\sqrt{N!}} \begin{vmatrix} \phi_1(\mathbf{r}_1) & \phi_1(\mathbf{r}_2) & \dots & \phi_1(\mathbf{r}_N) \\ \phi_2(\mathbf{r}_1) & \phi_2(\mathbf{r}_2) & \dots & \phi_2(\mathbf{r}_N) \\ \vdots & \vdots & \ddots & \vdots \\ \phi_N(\mathbf{r}_1) & \phi_N(\mathbf{r}_2) & \dots & \phi_N(\mathbf{r}_N) \end{vmatrix} \quad (2.30)$$

where $1/\sqrt{N!}$ is a normalisation factor. To illustrate this, consider a two-electron system with single-particle wavefunctions $\phi_1(\mathbf{r})$ and $\phi_2(\mathbf{r})$. The Slater determinant for this system would be:

$$\Psi^{HF}(\mathbf{r}_1, \mathbf{r}_2) = \frac{1}{\sqrt{2}} \begin{vmatrix} \phi_1(\mathbf{r}_1) & \phi_1(\mathbf{r}_2) \\ \phi_2(\mathbf{r}_1) & \phi_2(\mathbf{r}_2) \end{vmatrix} = \frac{1}{\sqrt{2}} [\phi_1(\mathbf{r}_1)\phi_2(\mathbf{r}_2) - \phi_1(\mathbf{r}_2)\phi_2(\mathbf{r}_1)] \quad (2.31)$$

Evidently, $\Psi^{HF}(\mathbf{r}_1, \mathbf{r}_2) = -\Psi^{HF}(\mathbf{r}_2, \mathbf{r}_1)$, which satisfies the antisymmetry principle.

2.3.2 The Hartree-Fock Equations

The Hartree-Fock equations are derived in a similar manner we addressed the Hartree equations. We first define the total energy with the Hartree-Fock wavefunction (Equation 2.30)

$$\begin{aligned} E^{HF}[\{\phi_i\}] &= \langle \Psi^{HF} | \hat{H} | \Psi^{HF} \rangle \\ &= \sum_i \langle \phi_i | \frac{\nabla^2}{2} + V_n(\mathbf{r}) | \phi_i \rangle \\ &\quad + \frac{1}{2} \sum_{i \neq j} \langle \phi_i \phi_j | \frac{1}{|\mathbf{r}_i - \mathbf{r}_j|} | \phi_i \phi_j \rangle \\ &\quad - \frac{1}{2} \sum_{i \neq j} \langle \phi_i \phi_j | \frac{1}{|\mathbf{r}_i - \mathbf{r}_j|} | \phi_j \phi_i \rangle \end{aligned} \quad (2.32)$$

Consecutively, using the variational principle, we derive the Hartree-Fock equations:

$$\left[-\frac{\nabla^2}{2} + V_n(\mathbf{r}) + V_i^H(\mathbf{r}) + \right] \phi_i(\mathbf{r}) - \sum_{j \neq i} \langle \phi_j | \frac{1}{|\mathbf{r}_i - \mathbf{r}_j|} | \phi_i \rangle \phi_j(\mathbf{r}) = \varepsilon_i \phi_i(\mathbf{r}) \quad (2.33)$$

Noticeably, Equation 2.33 has an extra term compared with the Hartree equation (Equation 2.28). This term is called the "exchange" term¹², and describes the effects of exchange between electrons. It is convenient to try to express the Hartree-Fock equations in a more compact form, so we define the single-particle and total densities as

$$\rho_i(\mathbf{r}) = |\phi_i(\mathbf{r})|^2 \quad (2.34)$$

$$\rho(\mathbf{r}) = \sum_i \rho_i(\mathbf{r}) \quad (2.35)$$

so the Hartree potential can be expressed as

$$V_i^H(\mathbf{r}) = \sum_{j \neq i} \int \frac{\rho_j(\mathbf{r}')}{|\mathbf{r} - \mathbf{r}'|} d\mathbf{r}' = \int \frac{\rho(\mathbf{r}') - \rho_i(\mathbf{r}')}{|\mathbf{r} - \mathbf{r}'|} d\mathbf{r}' \quad (2.36)$$

Therefore, the single-particle exchange density can be constructed as

$$\rho_i^X(\mathbf{r}, \mathbf{r}') = \sum_{j \neq i} \frac{\phi_i(\mathbf{r}') \phi_i^*(\mathbf{r}) \phi_j(\mathbf{r}) \phi_j^*(\mathbf{r}')}{\phi_i(\mathbf{r}) \phi_i^*(\mathbf{r})} \quad (2.37)$$

Finally, the Hartree-Fock equations take the form

$$\left[-\frac{\nabla^2}{2} + V_n(\mathbf{r}) + V_i^H(\mathbf{r}) + V_i^X(\mathbf{r}) \right] \phi_i(\mathbf{r}) = \varepsilon_i \phi_i(\mathbf{r}) \quad (2.38)$$

where V_i^X stands for the exchange potential

$$V_i^X(\mathbf{r}) = - \int \frac{\rho_i^X(\mathbf{r}, \mathbf{r}')}{|\mathbf{r} - \mathbf{r}'|} d\mathbf{r}' \quad (2.39)$$

2.4 Density Functional Theory

Hello

2.4.1 First Hohenberg-Kohn Theorem

2.4.2 Second Hohenberg-Kohn Theorem

2.4.3 Kohn-Sham Equations

2.4.4 Exchange-Correlation Functionals

2.5 Ab initio Molecular Dynamics

2.5.1 Born-Oppenheimer Molecular Dynamics

2.5.2 Car-Parrinello Molecular Dynamics

2.6 Machine Learning Force Fields

2.7 Computational Implementation in VASP

2.7.1 Plane Wave Basis Set

2.7.2 K-Point Sampling and Cutoff Energy

2.7.3 Pseudopotentials

2.8 Density of States

Chapter 3

Methodology

Chapter 4

Results & Discussion

4.1 My results

Hello

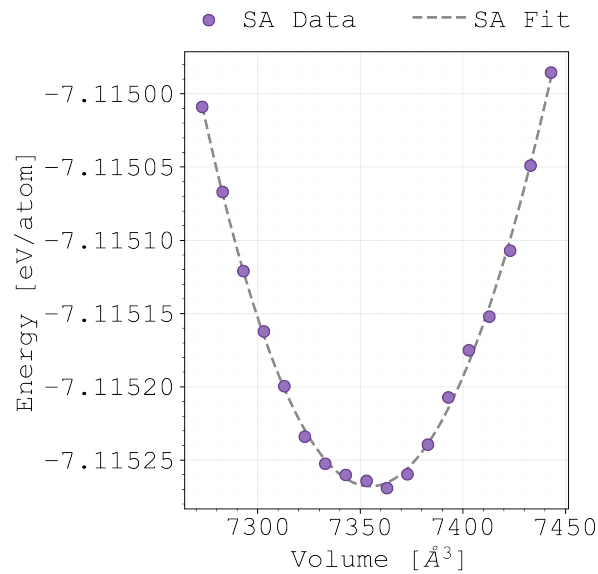


Figure 4.1: A schematic representation of the DFT formalism. The many-body wavefunction is replaced by a single-particle wavefunction, which is used to calculate the electron density. The electron density is then used to calculate the total energy of the system. Adapted from¹⁰.

Bibliography

- [1] Paulo J. M. Monteiro, Sabbie A. Miller, and Arpad Horvath. “Towards Sustainable Concrete”. In: *Nature Materials* 16.7 (July 2017), pp. 698–699. ISSN: 1476-4660. DOI: 10.1038/nmat4930. (Visited on 03/16/2025).
- [2] Henri Van Damme. “Concrete Material Science: Past, Present, and Future Innovations”. In: *Cement and Concrete Research*. SI : Digital Concrete 2018 112 (Oct. 2018), pp. 5–24. ISSN: 0008-8846. DOI: 10.1016/j.cemconres.2018.05.002. (Visited on 03/16/2025).
- [3] P. Kumar Mehta and Paulo J. M. Monteiro. “Introduction”. In: *Concrete: Microstructure, Properties, and Materials*. 4th Edition. New York: McGraw-Hill Education, 2014. ISBN: 978-0-07-179787-0.
- [4] Styliani Papatzani, Kevin Paine, and Juliana Calabria-Holley. “A Comprehensive Review of the Models on the Nanostructure of Calcium Silicate Hydrates”. In: *Construction and Building Materials* 74 (Jan. 2015), pp. 219–234. ISSN: 0950-0618. DOI: 10.1016/j.conbuildmat.2014.10.029. (Visited on 03/16/2025).
- [5] Katerina Ioannidou et al. “Mesoscale Texture of Cement Hydrates”. In: *Proceedings of the National Academy of Sciences* 113.8 (Feb. 2016), pp. 2029–2034. DOI: 10.1073/pnas.1520487113. (Visited on 01/16/2025).
- [6] Mohammad Javad Abdolhosseini Qomi, Mathieu Bauchy, and Roland J.-M. Pellenq. “Nanoscale Composition-Texture-Property Relation in Calcium-Silicate-Hydrates”. In: *Handbook of Materials Modeling: Applications: Current and Emerging Materials*. Ed. by Wanda Andreoni and Sidney Yip. Cham: Springer International Publishing, 2020, pp. 1761–1792. ISBN: 978-3-319-44680-6. DOI: 10.1007/978-3-319-44680-6_128. (Visited on 09/24/2024).
- [7] Ashraf A. Bahraq et al. “Molecular Simulation of Cement-Based Materials and Their Properties”. In: *Engineering* 15 (Aug. 2022), pp. 165–178. ISSN: 2095-8099. DOI: 10.1016/j.eng.2021.06.023. (Visited on 09/17/2024).
- [8] Emmy M. Foley, Jung J. Kim, and M. M. Reda Taha. “Synthesis and Nano-Mechanical Characterization of Calcium-Silicate-Hydrate (C-S-H) Made with 1.5 CaO/SiO₂ Mixture”. In: *Cement and Concrete Research* 42.9 (Sept. 2012), pp. 1225–1232. ISSN: 0008-8846. DOI: 10.1016/j.cemconres.2012.05.014. (Visited on 06/05/2025).

- [9] Mohammad Javad Abdolhosseini Qomi, Franz-Josef Ulm, and Roland J.-M. Pellenq. “Physical Origins of Thermal Properties of Cement Paste”. In: *Physical Review Applied* 3.6 (June 2015), p. 064010. DOI: 10.1103/PhysRevApplied.3.064010. (Visited on 09/11/2024).
- [10] F. Giustino. *Materials Modelling Using Density Functional Theory: Properties and Predictions*. Oxford University Press, 2014. ISBN: 978-0-19-966244-9.
- [11] D.S. Sholl and J.A. Steckel. *Density Functional Theory: A Practical Introduction*. Wiley, 2023. ISBN: 978-1-119-84086-2.
- [12] E. Kaxiras. *Atomic and Electronic Structure of Solids*. Cambridge University Press, 2003. ISBN: 978-0-521-81010-4.
- [13] R.M. Martin, L. Reining, and D.M. Ceperley. *Interacting Electrons*. Cambridge University Press, 2016. ISBN: 978-0-521-87150-1.
- [14] T. Helgaker, P. Jorgensen, and J. Olsen. *Molecular Electronic-Structure Theory*. Wiley, 2014. ISBN: 978-1-119-01955-8.
- [15] D. Feng and G. Jin. *Introduction to Condensed Matter Physics, Volume 1*. World Scientific Publishing Company, 2005. ISBN: 978-981-310-219-4.
- [16] D. R. Hartree. “The Wave Mechanics of an Atom with a Non-Coulomb Central Field. Part I. Theory and Methods”. In: *Mathematical Proceedings of the Cambridge Philosophical Society* 24.1 (Jan. 1928), pp. 89–110. ISSN: 1469-8064, 0305-0041. DOI: 10.1017/S0305004100011919. (Visited on 07/10/2025).
- [17] V. Fock. “Näherungsmethode zur Lösung des quantenmechanischen Mehrkörperproblems”. In: *Zeitschrift für Physik* 61.1 (Jan. 1930), pp. 126–148. ISSN: 0044-3328. DOI: 10.1007/BF01340294. (Visited on 07/10/2025).